Determination of Aquifer System Using Resistivity Method in Pekalongan City and Surrounding Areas, Central Java, Indonesia

Meitharisha F. Hasani[1,2(✉)], Heru Hendrayana[1], and Ahmad Taufiq[2]

[1] Geological Engineering Department, Universitas Gadjah Mada, Yogyakarta, Indonesia
meitharishafakhdiyarhasani@mail.ugm.ac.id
[2] Ministry of Public Works and Housing, Jakarta, Indonesia

Abstract. The increasing population growth and rapid development of Pekalongan in recent years have caused an increase in clean water needs that cannot be fulfilled from surface water due to pollution problems, so people prefer to use groundwater. Therefore, it is necessary to determine the aquifer system to know groundwater sustainability in this area. This study investigates subsurface lithology and aquifer layer thickness to determine the aquifer system. The investigation determined the subsurface lithology using the 1 Dimension Electrical Resistivity method with Schlumberger Configuration. Based on the investigation results, the rock layers in the northern part have resistivity values below 3 Ωm and 11–60 Ωm. The value is predicted by the loose and unconsolidated materials derived from the river and coastal deposits, predominantly sand-clay grain-sized. This layer is interpreted as the primary aquifer in the northern part. The other layer in the northern part, with a resistivity value of 3–10 Ωm, is interpreted as sandy clay and acts as an aquiclude. A layer with a resistivity value of 11–60 Ωm in the south is tuff sand. The tuff sand originates from volcanic rock debris and acts as an aquifer. The layer with a resistivity value of 3–10 Ωm is interpreted as a tuff clay. The tuff clay acts as an aquiclude layer. The layer with a resistivity value of more than 60 Ωm is known as the tuff breccia. The layer is an aquitard and base of the aquifer system.

Keywords: Resistivity Method · Subsurface Lithology · Aquifer System

1 Introduction

Pekalongan is one of the cities on the North Coast of Java Island, which has experienced rapid development in recent years. The industry's rapid growth is mainly in the batik industry, so Pekalongan is famous as the City of Batik. Also, it improves other sectors such as tourism, agriculture, trade, etc. In addition, Pekalongan also experienced a significant increase in population growth. In 2017 the total population of Pekalongan City was 301,870 people, then increased in 2021 to 308,310 people [1]. The development and population growth have led to an increasing need for clean water. The groundwater fulfills the clean water need in Pekalongan because of the limited surface water. Moreover,

N. I. Inda et al. (Eds.): ISST 2022, APR 7, pp. 100–108, 2023.
https://doi.org/10.2991/978-94-6463-228-6_12

groundwater in Pekalongan has better water quality due to pollution problems in surface water. The high demand for groundwater utilization causes the necessity of knowing the aquifer system condition in the research area. Therefore, the research aims to conduct aquifer thickness and groundwater potential to determine how the groundwater aquifer system in the Pekalongan area and its surroundings uses the geoelectric method.

One way to find out and determine how the aquifer system in the study area is to find out subsurface conditions using the geoelectric method. The geoelectric method is used to acquire the rock type's resistivity value related to its physical parameters, such as porosity, permeability, and water saturation degree [2]. In comparison, the geoelectrical investigation that is considered the most efficient and effective for groundwater is the resistivity method investigation. From the resistivity results, the depth of the aquifer, stratigraphy, and aquifer thickness can be obtained [3]. Regarding the arrangements of potential and current electrodes, the configuration types include Schlumberger, Wenner, and Dipole-Dipole. The Schlumberger configuration is frequently used for groundwater investigations for alluvium and solid rock area [4].

The study was conducted in the Pekalongan area and its surroundings as a part of the Pekalongan-Pemalang Groundwater Basin. In the study area, the geomorphological consists of an area with an altitude of fewer than 15 m above sea level as the plain morphology in the northern part that extends from west to east. The plain morphology occupies almost 60% of the study area. Then the slope morphology in the middle to southern parts with an altitude between 13–238 m above sea level. This slope morphology is considered a recharge area for the flatter part [5]. For geological conditions, the research area based on regional geology consists of formations sorted from old to young: The Damar Formation (QTd) in the eastern and western parts of the local consisting of tuff sandstone lithology, tuff claystone, and volcanic breccia. Alluvial Fan (Qf) in the middle to the southern part of the study area is rock debris from older volcanic rocks. Alluvial deposits (Qa) residing in the plain area. It is the result of river and beach deposits with loose and unmixed materials with gravel, sand, silt, and clay grain size [6].

Influenced by the geomorphological and geological conditions, it is known that the movement of groundwater from the Strato volcano groundwater region in the south to the plain groundwater region in the northern part bordering the Java Sea [5].

2 Methodology

The geoelectrical investigation method in this research is the VES (Vertical Electrical Sounding) or 1 Dimension resistivity method. The investigation is used to obtain the subsurface vertical resistivity values distribution. This method is applied to rock formations or horizontal deposits [7]. The measurement result is the resistivity value and depth of the layers. The interpreted log of the results consists of a series of 1D horizontal layers. The measurement principle of this method is to pass a current through two current electrodes and measure the magnitude of the voltage between two potential electrodes. Finally, the present value and voltage are used to calculate the resistivity value [8]. The resulting resistivity value is a pseudo-resistivity formulated as follows:

$$\rho_a = K\frac{\Delta V}{I};\ R\frac{\Delta V}{I} \tag{1}$$

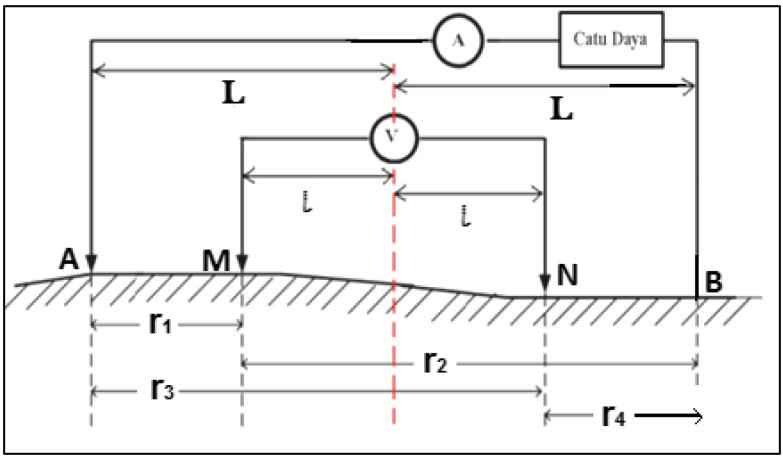

Fig. 1. Electrode Arrangement with Schlumberger Configuration [8, 10]

where the geometric factor is symbolized with K, ΔV is voltage, R is resistance, and I is the current flows between the electrodes [9]. This study uses Schlumberger Configuration, which was chosen because the penetration was deep enough to reach 1/5 of the spacing distance of the current electrode [8]. Schlumberger configuration electrode arrangement as seen in Fig. 1 where L is the space that separated the current electrodes and l is the spacing among the potential electrodes. After obtaining the pseudo-resistivity value, data processing is carried out using the IPI2win Application to get a 1D resistivity log. The 1D logs are then interpreted from the resistivity value of each layer and correlated with subsurface data from previous studies, such as bore log data.

In this study, the resistivity measurement was conducted at eight sounding points. The sounding point was chosen to deliver a review of the study area's subsurface condition. Measurements are carried out using an Ares-type Resistivitymeter tool with a stretch length of 200 m at each sounding point—the points of the resistivity measurement location as shown in Fig. 2.

3 Results and Discussion

The measurements taken at the study area obtained current and potential values using a Resistivity meter. Then data processing is carried out using IPI2win software. The data processing results are from resistivity values (Ωm) to depth (m) in the form of 1D log graphs and tables at eight measurement points. The resistivity value obtained was then correlated with previous data, such as log bore data and regional geological data. After correlation, subsurface lithological interpretation is carried out to define the aquifer systems. The cross-section profile of the resistivity values interpretation is divided into two cross-sections based on the location and formation of rocks in regional geology. The north cross-section (points R9, R10, and R16) and the south cross-section (points R11, R12, R13, R14 and R15).

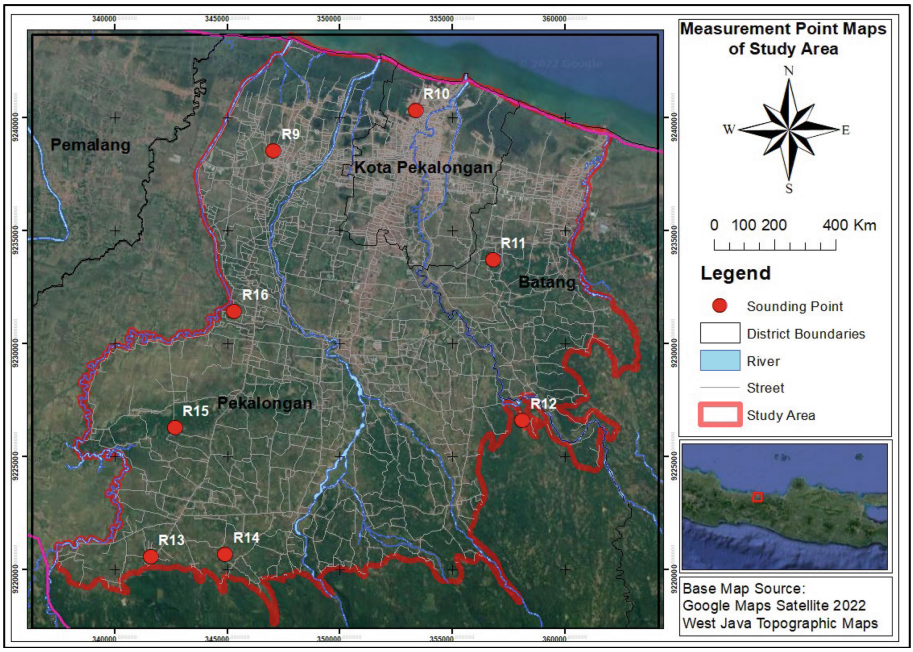

Fig. 2. Resistivity Measurement Location Maps of Study Area

3.1 North Cross Section

The rock layer cross-section from the resistivity measurements at points R9, R10, and R16 in the northern part is shown in Fig. 3. The R9 point profile obtained a depth of up to ±81 m. First, a clay sand stratum with a resistivity rate of 0.187 Ωm to 35.1 Ωm was observed at a depth of 0–23 m. The clay sand stratum thickness is 23 m—Sandy clay-clay with a resistivity rate of 0.976 Ωm–5.52 Ωm. The layers are 23–71.2 m below the surface, with a thickness of 48.2 m. Under the sandy clay stratum, there is a clay-sand stratum with a resistivity of 0.064 Ωm containing brackish water. The layers locate at depths of 71.2 m to 81.2 m from the surface, with a thickness of ±10 m.

Point R10 reached a maximum depth of ±77.7 m, and the resistivity log showed a clay sand stratum with a resistivity rate between 0.37 Ωm to 12.7 Ωm at a depth of 0–31.7 m below the surface with a thickness of 31.7 m. Next is a sandy clay-clay stratum with a resistivity rate of 6.33 Ωm at a depth of 31.7–39.7 m under the surface with a thickness of 8 m. Then beneath the sandy clay stratum is a clay sand containing brackish water with a resistivity rate of 0.0176 Ωm–0.184 Ωm at a depth of 39.7–77.7 m under the surface with a thickness of ±38 m.

Point R16 obtained a depth of up to ±88.6 m. First, the resistivity logs show a clay sand stratum with a resistivity rate of 0.61 Ωm–22.1 Ωm at a depth of 0–11.7 m from the surface with a thickness of 11.7 m. Next is a sandy clay stratum with a resistivity rate of 5.28–9.97 Ωm at a depth of 11.7–21.6 m under the surface with a thickness of 9.9 m. Finally, after the sandy clay, clay sand contains brackish water with a resistivity

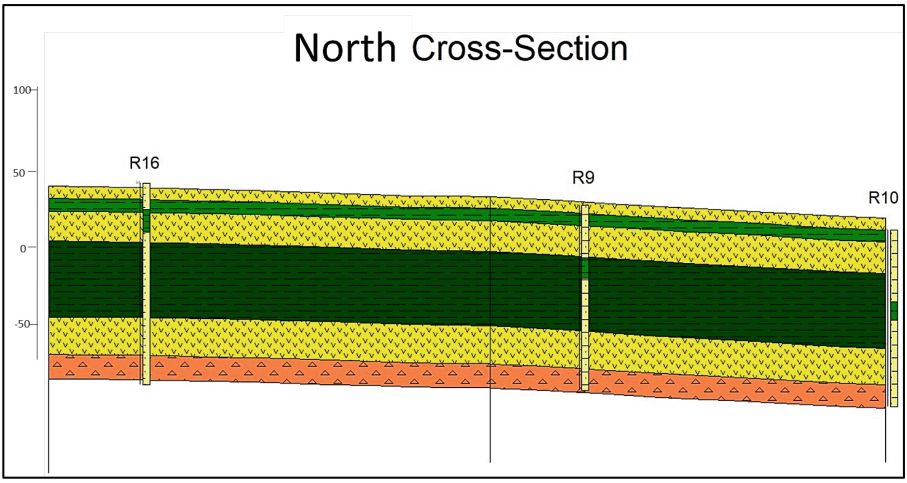

Fig. 3. North Cross Section of Study Area.

rate of 0.822 Ωm–70.9 Ωm at a depth of 21.6–88.6 m under the surface with a thickness of ±67 m.

3.2 South Cross Section

Figure 4 shows cross-sections of rock layers and resistivity measurements at points R11, R12, R13, R14, and R15, occupying the middle to the south of the study area. The R11 point profile reached a depth of up to ±82.6 m and showed a tuff sand stratum with a resistivity rate of 6.02 Ωm–83.2 Ωm at a depth of 0–6.04 m from the surface with a thickness of 6.04 m. Then a tuff clay with a resistivity rate of 3.26 Ωm–10.4 Ωm at a depth of 6.04–11.3 m with a thickness of 5.26 m. After the tuff clay, there is a tuff sand stratum with a resistivity rate of 42.2 Ωm at a depth of 11.3–25.6 m with a thickness of ±14.3 m. After the tuff sand, there is a tuff clay stratum with a resistivity rate of 0.757 Ωm at a depth of 25.6–59 m beneath the surface with a thickness of 33.4 m. Next is a tuff sand lithology with a resistivity rate of 22.2 Ωm at 59–72.6 m under the surface with a thickness of 13.6 m. In the end, the bottom layer with a significant resistivity value of 208 Ωm was obtained, then described as a tuff breccia at a depth of 72.6–82.6 m beneath the surface with a thickness of ±10 m.

Point R12 reached a maximum depth of ±86.4 m and showed a layer of gravel sand with a resistivity rate of 4.69 Ωm–248 Ωm at a depth of 0–2.69 m under the surface. The layer thickness is 2.69 m. Then a layer of tuff clay with a resistivity rate of 1.99 Ωm–4.18 Ωm at a depth of 2.69–6.95 m with a thickness of 4.26 m. Next is a tuff sand stratum with a resistivity rate of 31.4 Ωm–52.2 Ωm at a depth of 6.95–22.1 m under the surface with a thickness of 15.15 m. After the tuff sand, there is a tuff clay stratum with a resistivity rate of 3.39 Ωm at a depth of 22.1–56.9 m from the surface with a thickness of 34.8 m. Next is the tuff sand stratum with a resistivity rate of 65.5 Ωm at a depth of 56.9–76.4 m with a thickness of 19.5 m. Finally, the basement layer is a tuff breccia

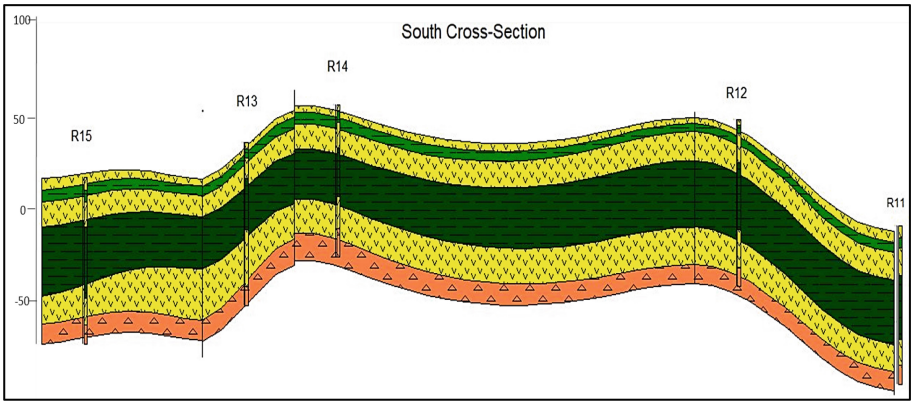

Fig. 4. South Cross Section of Study Area.

with a resistivity rate of 276 Ωm at a depth of 76.4–86.4 m from the surface. The layer thickness is ±10 m.

Point R13 obtained a depth of ±84.7 m and showed a layer of gravel sand with a resistivity rate of 120 Ωm–1528 Ωm at a deepness of 0–3.54 m from the surface with a thickness of 3.54 m. Then a tuff clay stratum with a resistivity rate of 4.14 Ωm–5.78 Ωm at a depth of 3.54–8.38 m under the surface with a thickness of 4.84 m. Beneath the tuff clay, there is a tuff sand-gravel sand stratum with a resistivity rate of 45 Ωm–124 Ωm at a deepness of 8.38–18.6 m from the surface with a thickness of 10.22 m. After that, a layer with a resistivity rate of 4.29 Ωm is a tuff clay. The layer is occupying at a depth of 18.6–45.5 m, with a layer thickness of 26.9 m. Next is a tuff sand layer with a resistivity value of 94.2 Ωm at a depth of 45.5–74.7 m below the surface with a thickness of 29.2 m. Finally, a tuff breccia was obtained in the base layer with a resistivity value of 1749 Ωm at a depth of 74.7–84.7 m under the surface. The layer thickness is ±10 m.

Point R14 obtained a depth of up to ±79.3 m and showed a tuff sand-gravel sand stratum with a resistivity rate of 39.6 Ωm–407 Ωm at a depth of 0–3.14 m under the surface with a thickness of 3.14 m. Then a tuff clay stratum with a resistivity rate of 3 Ωm–14.5 Ωm at a deepness of 3.14–9.34 m under the surface with a thickness of 6.2 m. Next, under the tuff clay layer, there is a layer of tuff sand with a resistivity value of 90.9 Ωm–96 Ωm at a depth of 9.34–22.6 m from the surface. The layer thickness is 13.26 m. Next, a tuff clay with a resistivity rate of 6.3 Ωm. The layer is at a depth of 22.6–48 m below the surface and a thickness of 25.4 m. After the tuff clay, a tuff sand stratum with a resistivity rate of 84.9 Ωm. The layers are placed at a depth of 48–64.3 m beneath the surface with a thickness of 16.3 m. The bottom layer of the measurement results is a tuff breccia with a resistivity rate of 1750 Ωm. The layer is located at a depth of 64.3–79.3 m under the surface with a thickness of ±15 m.

Point R15 obtained a depth of up to ±86.4 m and showed a tuff sand stratum with gravel sand inserts with a resistivity rate of 10.3 Ωm–150 Ωm at a depth of 0 m–6.55 m under the surface with a thickness of 6.55 m. Then a layer of tuff clay with a resistivity rate of 3.51 Ωm at a depth of 6.55 m–12.9 m from the surface with a thickness of 6.35 m. Next, under the tuff clay layer, there is a tuff sand stratum with a resistivity rate

of 40.6 Ωm–69 Ωm at a depth of 12.9 m–25.7 m beneath the surface with a thickness of 12.8 m. After that, a tuff clay with a resistivity rate of 3 Ωm. The layer is placed at a deepness of 25.7 m–62.8 m under the surface with a thickness of 37.1 m. Next is a tuff sand layer with a resistivity rate of 59.7 Ωm at 62.8 m–76.4 m from the surface with a thickness of 13.6 m. The basement layer is a tuff breccia with a resistivity rate of 407 Ωm at a depth of 76.4 m–86.4 m beneath the surface with a thickness of ±10 m.

3.3 Aquifer System of Study Area

Based on the resistivity results associated with log bore data, it can be interpreted that there are two types of aquifers. First, there are unconfined and confined aquifers. The unconfined aquifer is laying on clay sand in the north with a thickness ranging from 11.7–31.7 m and in the southern part with its main layer of tuff sand and sectionally gravel sand with a thickness ranging from 2.69 to 6.55 m. Then under the layer that becomes an unconfined aquifer, there is an aquiclude layer in the lithology of sandy clay, clay, and tuff clay with a thickness of between 4.26–48.2 m. A confined aquifer is after the aquiclude layer with clay sand lithology in the northern part and tuff sand in the southern part with a thickness varying between 10.22–67 m. After the confined, a layer of tuff breccia as an aquitard with a thickness of ±10 m and so on.

Previously, measurements of groundwater levels from dug wells in the research area have obtained the depth of groundwater levels varying from the lowest, −1.24 masl, located in the north part, to the highest, 160.31 masl, situated in the hilly area in the south, with an average groundwater level of 18.60 masl. The groundwater flow movement is from the south part towards the north part of the study area. According to log bore data, the hydraulic conductivity varies from 0.00056–0.0000392 m/s. The transmissivity varies from 9.3–247.13 m^2/day with a specific capacity of 0.59 to 0.07 l/s/m.

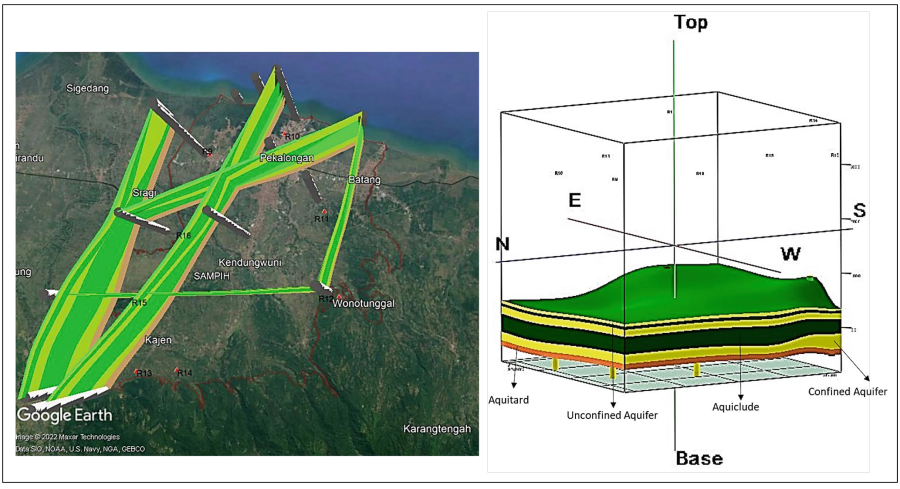

Fig. 5. Fence Diagram and Aquifer System in Study Area.

4 Conclusions

Based on the resistivity measurements, the lithology of the study area consists of clay sand, sandy clay, and clay. It is derived from the Alluvial Deposit formation in the northern part of the study area. Meanwhile, the southern part consists of the lithologies of tuff sand, tuff clay, and local gravel sand, which are known to be derived from the Alluvium fan formation from the older volcanic rock debris in the study area. Then the layer with the significant resistivity value is interpreted as a tuff breccia. The tuff breccia derived from the Damar formation.

The aquifers system consists of unconfined and confined aquifers. The unconfined aquifer consists of clay sand in the north and tuff sand, locally gravel sand in the south. The confined aquifer consists mainly of tuff sand with gravel sand inserts in the northern part thickening to the southern part. There are two aquiclude layers consisting of sandy clay-clay and one layer of tuff breccia as an aquitard.

References

1. Unknown, Pekalongan Municipality in Figures 2022, Publication Number: 33750.2202, Statistics of Pekalongan Municipality (2022).
2. Simpen, I.N.: Metoda Geolistrik, Civil Engineering Departments, Faculty of Engineering, Universitas Udayana (2015).
3. Mohamaden, M., et al.: Application of electrical resistivity method for groundwater exploration at the Moghra area, Western Desert, Egypt, (The Egyptian Journal of Aquatic Research) pp. 261–268. (2016).
4. Rolia, E., Sutjiningsih, D.: Application of Geoelectric Method for Groundwater Exploration from Surface (A Literature Study), AIP Conference Proceedings, 020018 (2018).
5. Effendi, A.T.: Hydrogeological Map of Indonesia 1:250.000 Sheet IV Pekalongan, Geological Agency, Bandung (1985).
6. Condon, W.H., et al.: Geological Map of Banjarnegara and Pekalongan Quadrangles Central Java, Indonesian Geological Agency, Bandung (1996).
7. Ernstson, K., Kirsch, R.: Metode Geolistrik, Geofisika Air Tanah: Alat untuk Hidrogeologi, p.84–117 (2006).
8. Reynolds, J.M.: An Introduction to Applied and Environmental Geophysics. New York: Jhon Geophysics in Hydrogeological and Wiley and Sons Ltd. (1997).
9. Loke, M.H.: 2D and 3D Electrical Imaging Surveys. England: Birmingham University (2004).
10. Anggara, A.D., Supriyadi, Priyantari, N.: Litology Identification of The Klanceng Site Using 1D Geoelectric Resistivity Method, BERKALA SAINSTEK, VII (2): 49–52 (2019).